Supporting information for

Edge-Centred Chirality Induced Enantiopure Square-Like Sulfonylcalix[4]arene-{Co^{II}_{16}} Cages for Selective (+)-/(-)-α-Pinene Adsorption

Ilia D. Shutilov,[a] Pavel A. Volodin,[b] Alexander S. Ovsyannikov,[a,*] Ilya M. Zinoviev,[c] Vladimir Yu. Guskov,[c] Daut R. Islamov,[d] Timur A. Mukhametzyanov,[b] Meijin Lin,[e] Pavel V. Dorovatovskii,[f] Georgy S. Peters,[f] Elizaveta S. Kulikova,[f] Vladimir A. Burilov,[b] Svetlana E. Solovieva[a], Igor S. Antipin[b]

[a] *Arbuzov Institute of Organic and Physical Chemistry, FRC Kazan Scientific Center, Russian Academy of Sciences, Arbuzova 8 str, Kazan, 420088, Russian Federation*

[b] *Kazan Federal University, Kremlevskaya 18 str, Kazan 420008, Russian Federation*

[c] *Ufa University of Science and Technology, Zaki Validi 32 str., Ufa 450076, Russian Federation*

[d] *Laboratory for structural analysis of biomacromolecules, FRC Kazan Scientific Center, Russian Academy of Sciences, Lobachevskogo 2/31 str., Kazan, 420111, Russian Federation*

[e] *College of Chemistry, Fuzhou University, Fuzhou, 350116, P. R. China*

[f] *National Research Center "Kurchatov Institute", Academician Kurchatov 1 pl., Moscow, 123182, Russian Federation*

**Corresponding author: osaalex2007@rambler.ru*

1. Experimental section

All chemicals were purchased from commercial suppliers and used without additional purification. Solvents were purified according to standard procedures.[1] The corresponding starting compounds (S)-(-)-1-phenylethylamine and (R)-(+)-1-phenylethylamine were purchased by Sigma Aldrich (USA) company with enantiomeric access more than 95.5%.

$^{1}H/^{13}C$ NMR spectra were recorded on AVANCE IITM 600/151MHz BRUKER BioSpin (Germany) with signals from residual protons of $CDCl_3$ as internal standard.

The MALDI TOF mass-spectra were recorded on an Ultraflex III TOF/TOF mass spectrometer (Bruker Daltonic GmbH, Bremen, Germany) operated in the linear mode with the registration of positively charged ions. 2,5-Dihydroxybenzoic acid (DHB) was used as a matrix.

High-resolution mass spectra for studied complexes with electrospray ionization (HRESI MS) were obtained on an Agilent iFunnel 6550 Q-TOF LC/MS (Agilent Technologies, Santa Clara, CA, USA). Carrier gas: nitrogen, temperature 300 °C, carrier flow rate 12.1 × min⁻1, nebulizer pressure 275 kPa, funnel voltage 3500 V, capillary voltage 500 V, total ion current recording mode, 100–3200 m/z mass range, scanning speed 7 spectra·s^{-1}.

Infrared spectra (IR) of milled crystalline samples in KBr pellets were recorded on a Tensor 27 Fourier-transform spectrometer (Bruker) in a range of 4000-400 cm^{-1} with an optical resolution of 4 cm^{-1} and an accumulation of 32 scans.

The X-ray powder diffraction pattern of quickly decomposing crystalline phase of **2-Dy** was studied at room temperature at the 'Belok/XSA' beamline station of the Kurchatov synchrotron radiation source, equipped with a Rayonix SX165 two-dimensional CCD detector (λ=0.7517 Å).[2, 3] The measurements were carried out at room temperature in the transmission geometry, the detector was located at a distance of 250 mm from the sample and 18˚ tilt angle to maximize the angular range. The diffraction pattern was converted to the one-dimensional form I (2θ) using azimuthal integration in the Dionis software,[4] with the use of the certified LaB_6 (NIST SRM 660a) as polycrystalline standard.

SAXS experiments were carried at BioMUR beamline station of the Kurchatov synchrotron radiation source[5,6] on an automated laboratory source small-angle X-ray diffractometer ''AMUR-K''[7] (Moscow, Russia), equipped with a DECTRIS Pilatus3 1M detector (λ=0.144 nm), positioned at a distance of 750 mm from the sample, , Kratky collimation system, and. One-dimensional scattering curves were obtained from 2D graphs using azimuthal integration in *Fit2D* software[8]. Further data processing, including particles size distribution calculations, were performed using the *ATSAS* software[9].

The circular dichroism (CD) spectra of obtained complexes were recorded in THF solution (C= $2.5 \cdot 10^{-4}$ M) on J-1500 CD spectropolarimeter (Jasco, Tokyo, Japan) in the wavelength range of 220–350 nm at room temperature in a rectangular quartz cuvette with 1 cm optical pathlength.

A TGA/DSC NETZSCH (Selb, Germany) STA449 F3 were used for the thermal analysis (thermogravimetry/differential scanning calorimetry) in which the variation of the sample mass as a function of temperature and the corresponding heats are recorded. An approximately 15 mg sample was placed in an Al crucible with a pre-hole on the lid and heated from 25 to 500°C. The same empty crucible was used as the reference sample. High-purity argon was used with a gas flow rate of 50mL/min. TGA measurement were performed at the heating rates of 5 K/min

Elemental analysis was performed on a EuroEA 3028-HT-OM Eurovector S.p.A. (Italy).

α-Pinene enantiomer adsorption was studied by inverse gas chromatography. A stainless steel column measuring 300×3 mm was filled with achiral styrene-divinylbenzene porous polymer (S-DVB, Dowex V503, Dow Chemicals, USA), modified by **SO_2CA-Co_4-1** or **SO_2CA-Co_4-2**. The cage:polymer mass ratio was 1:100 was used. Upon the deposition the cage powder sample was dissolved in chloroform, mixed with S-DVB particles and evaporated to dryness upon the vigorous stirring in vacuum. The column was preliminary conditioned at 95 ˚C overnight. GC studies were carried out on a Krystall 5000.2 gas chromatograph (Khromatek, Yoshkar-Ola, Russia) equipped with a thermal conductivity detector. The column temperature ranged from 85 to 95 ˚C. At lower

temperatures the quasi-equilibrium state in chromatographic column didn't reach. The temperature of the injector and detector was 200 ˚C. The helium carrier gas flow rate for the α-pinene enantiomers was 30 mL·min^{-1}. To obtain adsorption isotherms, inverse gas chromatography was used under finite concentration conditions: samples were injected as liquids with a known volume ranging from 2 to 5 ml.

The number of adsorbed α-pinene molecules and the partial pressure of enantiomer vapors were calculated according to Kiselev and Yashin[10]:

$$a = \frac{nS_{ads}}{mS} \tag{1}$$

$$p = \frac{nh}{Sw}RT \tag{2}$$

n is the injected α-pinene amount, mmol; S_{ads} is the adsorption area, mV·s; S is the peak area, mV·s; m is the modified by **SO_2CA-Co_4-1** or **SO_2CA-Co_4-2** styrene-divinilbenzene porous polymer mass in the chromatographic column, g; h is the peak height, mV; and ω is the carrier gas flow rate, ml·s$_{-1}$.

In order to fit experimental data, a number of isotherm model were used. The form of isotherm obtained was corresponded to BET type I. So, it could be approximate by Langmuir equation (3):

$$\frac{p}{a} = \frac{1}{a_m K_L} + \frac{p}{a_m} \tag{3}$$

where a_m is the monolayer capacity, μmol·g^{-1}; K_L is the Langmuir constant, Pa^{-1}. Since the cage size is 14 Å, the Dubinin and Radushevich equation [11,12] was used:

$$lna = lnW_0 - \frac{R^2T^2}{E^2} \cdot ln\left(\frac{p}{p_s}\right)^2 \tag{4}$$

W_0 – micropore volume, ml·g^{-1}; E – characteristic energy, kJ·mol^{-1}. Fowler-Guggenheim model was used to obtain lateral interactions energy values:

$$ln\left[\frac{p(1-\theta))}{\theta}\right] = -lnK_{FG} + \frac{2b\theta}{RT} \tag{5}$$

where:

$$\theta = \frac{q_e}{q_m} \tag{6}$$

K_{GF}: Fowler-Guggenheim constant, Pa^{-1}; b: interaction energy between adsorbed molecules, kJ·mol^{-1}.

Toth equation was used for estimating the adsorption heterogeneity:

$$\theta = \frac{K_T p}{\left[1 + (K_T p)^n\right]^{1/n}} \tag{7}$$

where K_T is the Toth constant, Pa^{-1}; and n is the heterogeneity parameter.

2. Synthesis of chiral V-shaped linkers supported on isophthalic acid platform

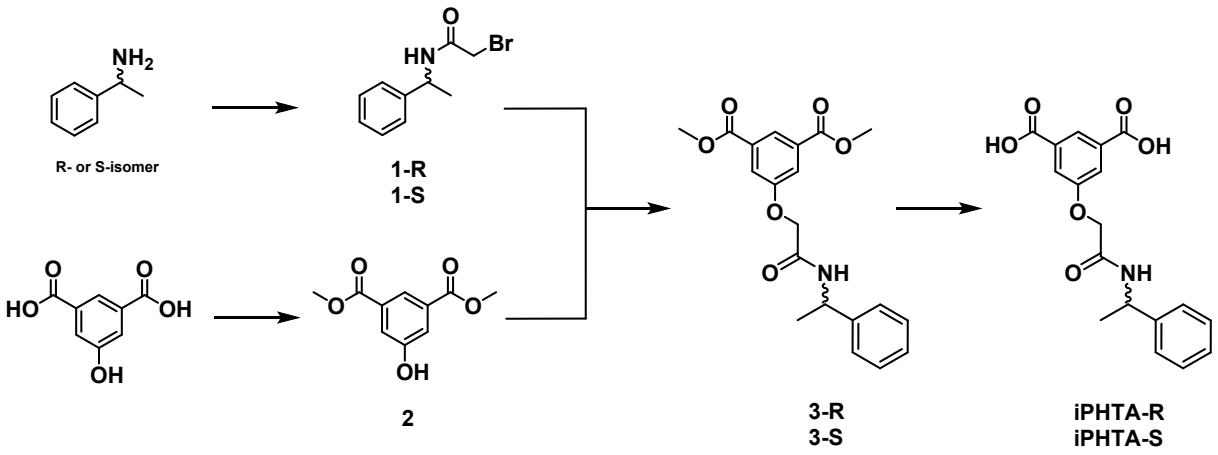

Scheme S1

*(R)/(S)-2-bromo-N-(1-phenylethyl)acetamide (**1-R/1-S**)*: Under inert atmosphere, a solution of bromoacetyl bromide (1.08 ml, 12.38 mmol) in absolute chloroform (50 ml) was mixed with K_2CO_3 (1.71 g, 12.38 mmol), followed by dropwise addition of chloroform solution (5 ml) containing dissolved *(R)/(S)*-phenylethylamine (1.05 ml, 8.25 mmol) at 0 °C. The resulting mixture was stirred at room temperature for 12 h. Then the organic phase was treated with a saturated water solution of Na_2SO_4 (50 ml) and washed 2 times by 100 ml of distilled water. The organic layer was collected and dried over anhydrous magnesium sulfate. After filtration, the organic solvent was evaporated to dryness, affording a product as a white powder (1.96 g, 98%). M_p 113.6 °C. ^{1}H NMR (400 MHz, $CDCl_3$) δ, *ppm*: 1.53 (3H, *d*, ^2J=6.8 Hz, CH_3), 3.88 (2H, *dd*, ^1J=14.0 Hz, CH_2), 5.04-5.17 (1H, *m,* CH), 7.27-7.41 (5H, *m*, CH_{Ar}). ^{13}C NMR (151 MHz, $CDCl_3$) δ, *ppm*: 56.48, 60.01, 109.56, 117.36, 119.36, 125.01, 128.63, 129.74, 135.60, 149.50, 151.15, 165.12. MALDI-MS, m/z: 298.9 $[M+K+H_2O]^+$ (m/z_{calc}: 299.2). IR (KBr, cm^{-1}) υ: 3264(s), 3061(m), 3025(w), 2977(m), 1648(s), 1548 (s) 1492(m), 1446(m), 1418(m), 1372(m), 1332(w), 1287(w), 1208(m), 1155(w), 1135(w), 1097(m), 1062(m), 1043(m), 968(m), 914(m), 790(w), 755(m), 698(m), 663(m), 591(m), 562(m), 509(m). Anal. Calc. for $C_{10}H_{12}BrNO$, %: C, 49.61; H, 5.00; N, 5.79. Found, %: C, 49.76; H, 5.06 N, 5.71.

*Dimethyl 5-Hydroxyisophthalate (**2**)* was synthesized following by the earlier reported procedure using esterification of 5-hydroxyisophthalic acid with methanol.[13] ^{1}H NMR (400 MHz, $CDCl_3$) δ, *ppm*: 3.95 (6H, *s*, CH_3) , 7.77 (2H, *s*, CH_{Ar}), 8.25 (1H, *s*, CH_{Ar})

*(R)/(S)-Dimethyl-5-(2-oxo-2-((1-phenylethyl)amino)ethoxy)isophthalate (**3-R/3-S**):* In a reaction flask (250 ml), sodium hydride (0.248 g, 6.20 mmol, 60 wt% in oil) was added to 5-hydroxydimethyl isophthalate 2 (1.00 g, 4.13 mmol) solution in absolute THF (100 ml) at room temperature under argon atmosphere upon stirring. The resulting mixture was heated up till 66 °C and a solution of (R)/(S)-2-bromo-N-(1-phenylethyl)acetamide (1,152 g, 4,758 mmol) **1** in absolute THF (20 ml) was added dropwise. The reaction mixture was refluxed for 3 h upon stirring under argon. The reaction was monitored using TLC (EA:petroleum ether = 1 : 2). The organic solvent was evaporated to dryness. The obtained residue was treated with H_2O (100 ml) and EA (70 ml) for extraction. The organic layer was collected and dried over magnesium sulfate. After filtration, the organic solvent was evaporated to dryness affording **3** as a white powder (1.52 g, 99%). M_p 103.0 °C. ^{1}H NMR (400 MHz, $CDCl_3$) δ, *ppm*: 1.55 (3H, *d*, ^2J=6.8 Hz, CH_3), 3.94 (6H, *s*, CH_3), 4.56 (2H, *dd*, ^1J=14.8 Hz, CH_2), 5.19-5.30 (1H, *m,* CH), 6.76 (1H, *d*, ^3J=8.4 NH), 7.24-7.37 (5H, *m*, CH_{Ar}), 7.76 (2H, *d*, ^4J=1.6 CH_{Ar}), 8.34 (H, *t*, ^4J=1.6 CH_{Ar}). ^{13}C NMR (101 MHz,

$CDCl_3$) δ, *ppm*: 60.61, 117.14, 118.86, 118,96, 128.24, 129.29, 131.66, 132.62, 136.14, 161.12, 166.16. MALDI-MS, m/z: 394.4 $[M+Na]^+$ (m/z_{calc}: 394.1); m/z: 410.5 $[M+K]^+$ (m/z_{calc}: 410.1). IR (KBr, cm^{-1}) υ: 3433(m), 3284(s), 3083(m), 2956(m), 2921(m), 1727(s), 1666(s), 1596(m), 1552(m), 1493(w), 1460(m), 1438(m), 1382(w), 1340(m), 1316(m), 1258(s), 1190(w), 1124(m), 1105(m), 1187(m), 1119(w), 996(m), 939(m), 913(w), 882(w), 785(w), 758(m), 723(m), 698(m), 671(w), 623(w), 573(w), 535(w). Anal. Calc. for $C_{20}H_{21}NO_6$, %: C, 64.68; H, 5.70; N, 3.77. Found, %: C, 64.57; H, 5.75; N, 3.82.

(R)/(S)-5-(2-oxo-2-((1-phenylethyl)amino)ethoxy)isophthalic acid (**iPHTA-R**/**iPHTA-S**): Compound **3** (1.40 g, 3.77 mmol) was dissolved in 1 M methanolic solution of NaOH (100 ml) and refluxed for 12 hours upon stirring. Then the solvent was removed in vacuum. A water solution of 0.1 M H_2SO_4 (200 ml) was poured into the flask. The precipitate was formed, filtered out and washed with water (3×20 ml) on the filter funnel. The obtained product as white powder was dried under vacuum conditions during 12 h (1.21 g, 94%). M_p 250.9 °C. ^{1}H NMR (600 MHz, DMSO-d_6) δ, *ppm*: 1.39 (3H, *d*, ^2J=4.0 Hz, CH_3), 4.68 (2H, *dd*, ^1J=9.6, CH_2), 4.97-5.03 (1H, *m,* CH), 7.18-7.21 (1H, *m*, CH_{Ar}) 7.25-7.33 (4H, *m*, CH_{Ar}), 7.69 (2H, *d*, ^4J=0.96 CH_{Ar}), 8.08 (H, *t*, ^4J=0.92 CH_{Ar}), 8.72 (1H, *d*, ^3J=5.4 NH), 13.26 (2H, *s*, COOH). ^{13}C NMR (101 MHz, DMSO-d_6) δ, *ppm*: 22.16, 47.65, 66.96, 119.43, 122.63, 125.94, 126.58, 128.16, 132.53, 144.22, 157.98, 166.24, 166.33. MALDI-MS, m/z: 342.2 $[M-H]^-$ (m/z_{calc}: 342.3). IR (KBr, cm^{-1}) υ: 3268(m), 3070(s), 2977(m), 2927(m), 1695(s), 1650(s), 1598(m), 1553(m), 1497(w), 1460(m), 1422 (m), 1338(m), 1277(m), 1316(m), 1130(m), 1106(m), 1074(m), 1023(w), 954(m), 910(m), 887(m), 759(m), 694(m), 664(w), 609(w), 580(w), 516(w). Anal. Calc. for $C_{18}H_{17}NO_6$, %: C, 62.97; H, 4.99; N, 4.08. Found, %: C, 63.05; H, 5.03; N, 4.05.

2.1 ^{1}H NMR characterization

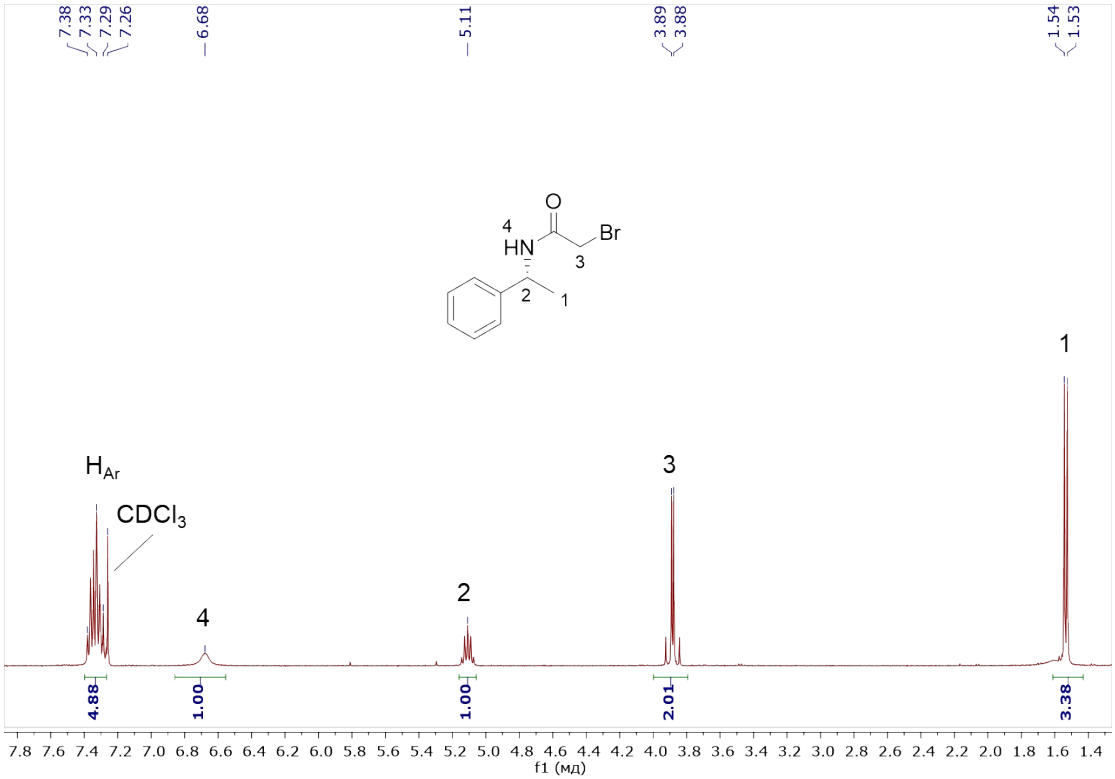

Figure S1. ^{1}H NMR spectrum for **1-R** ($CDCl_3$, 400 MHz, 25 °C).

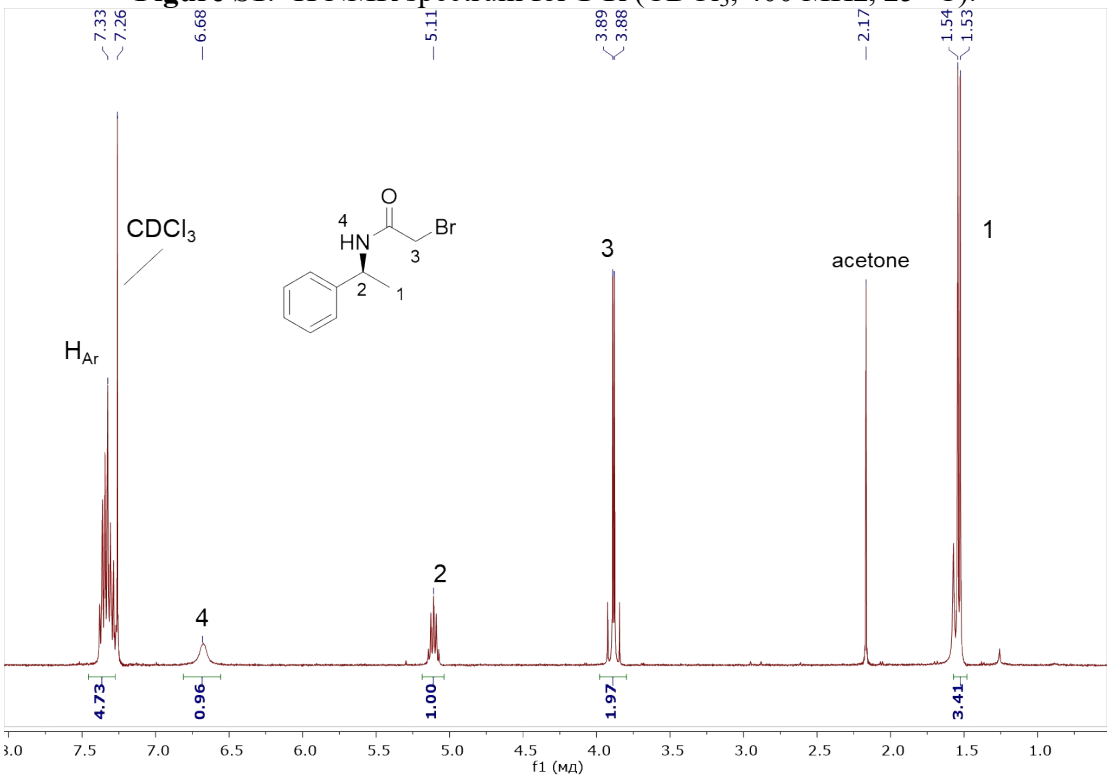

Figure S2. ^{1}H NMR spectrum for **1-S** ($CDCl_3$, 400 MHz, 25 °C).

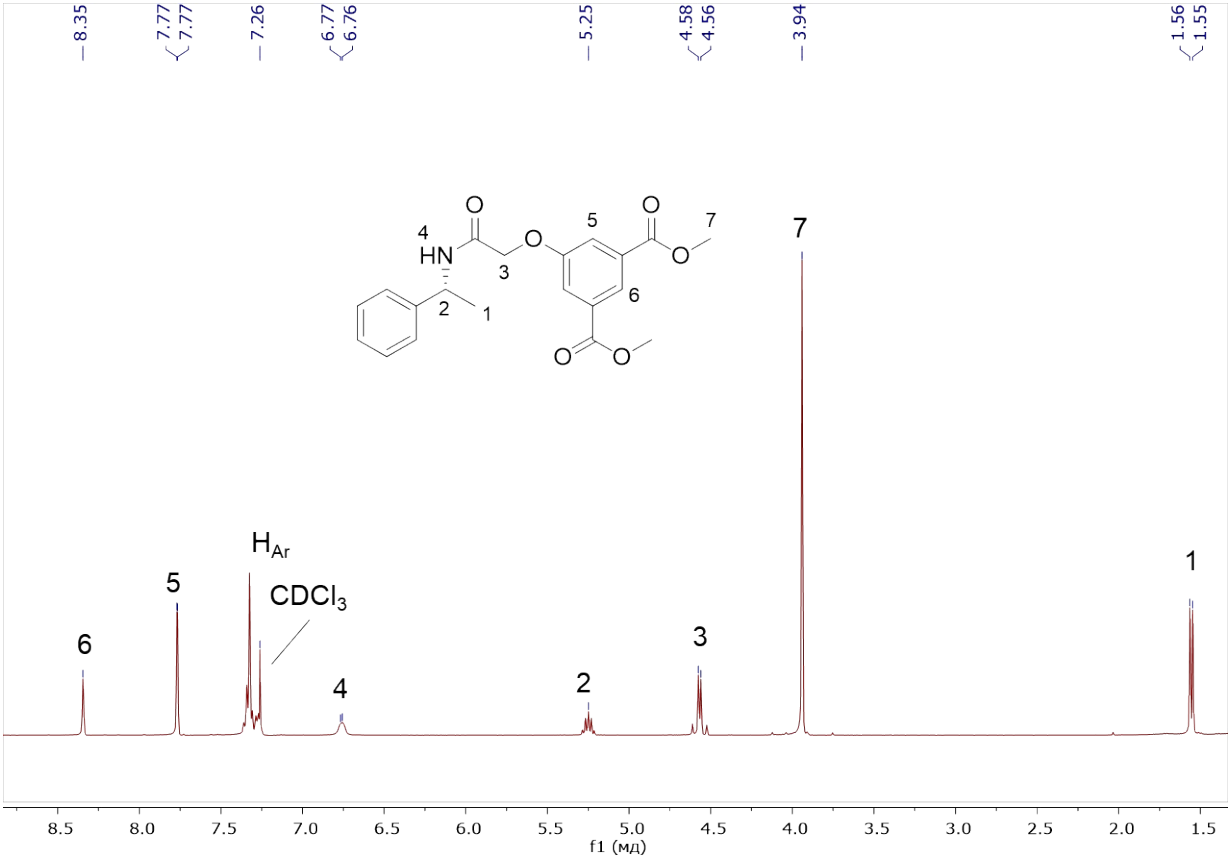

Figure S3. ^{1}H NMR spectrum for **3-R** ($CDCl_3$, 400 MHz, 25 °C).

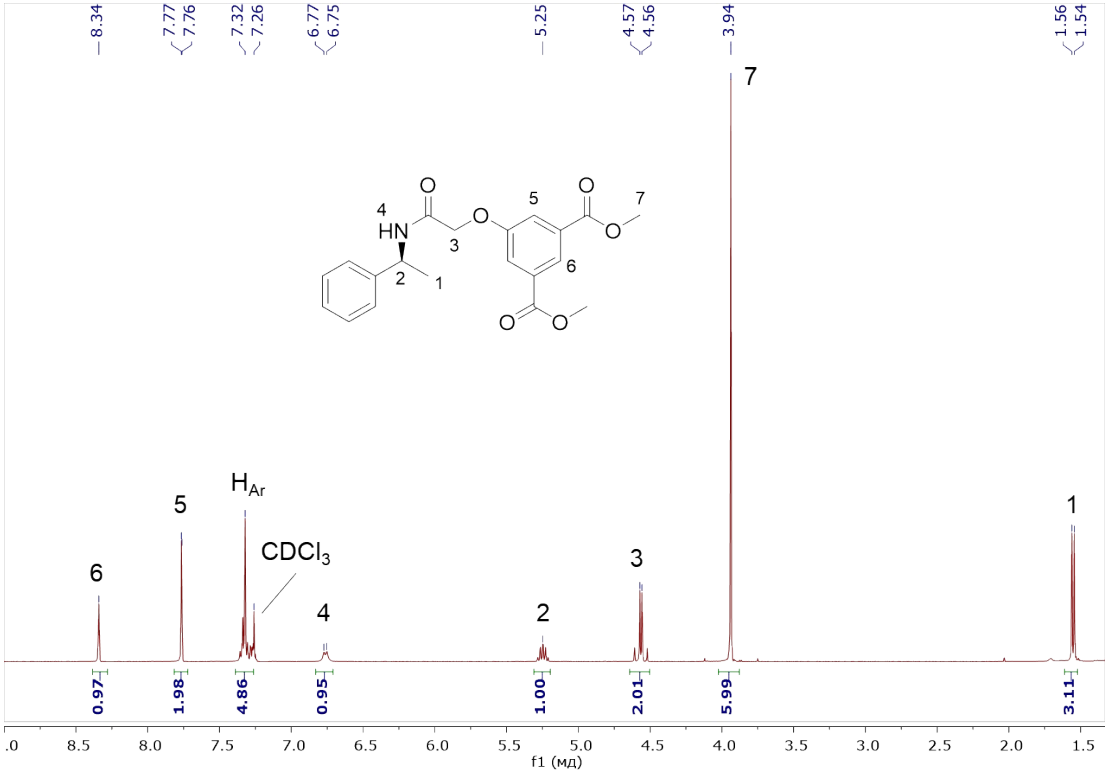

Figure S4. ^{1}H NMR spectrum for **3-S** ($CDCl_3$, 400 MHz, 25 °C).

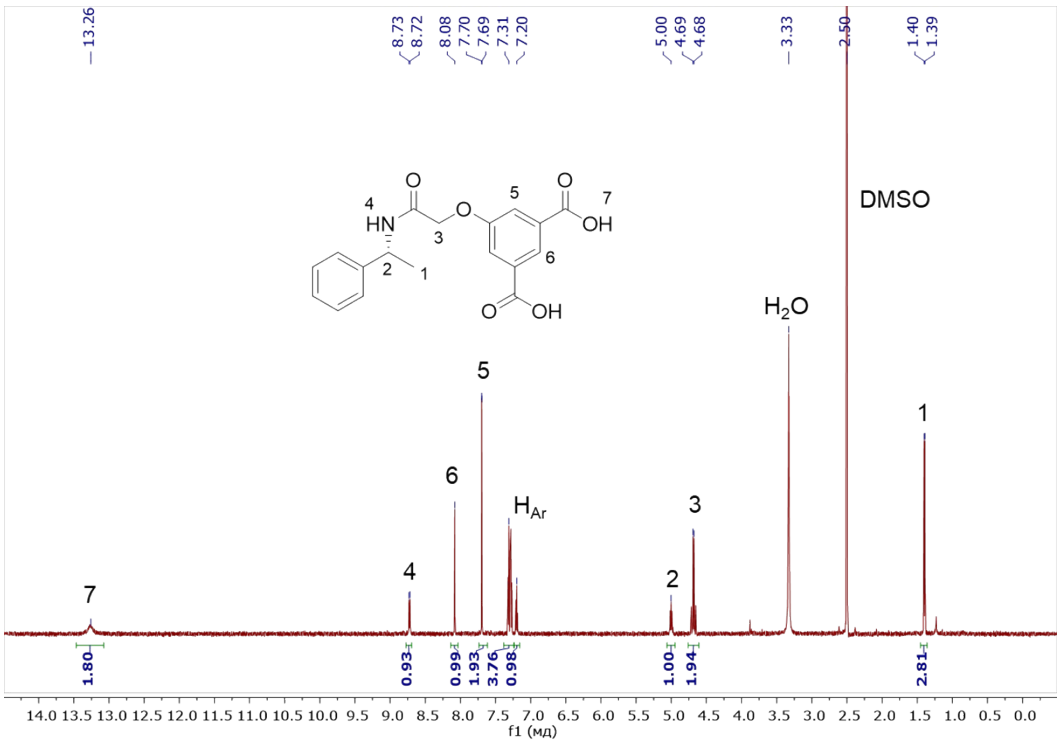

Figure S5. ^{1}H NMR spectrum for **iPHTA-R** (DMSO-d_6, 600 MHz, 25 °C).

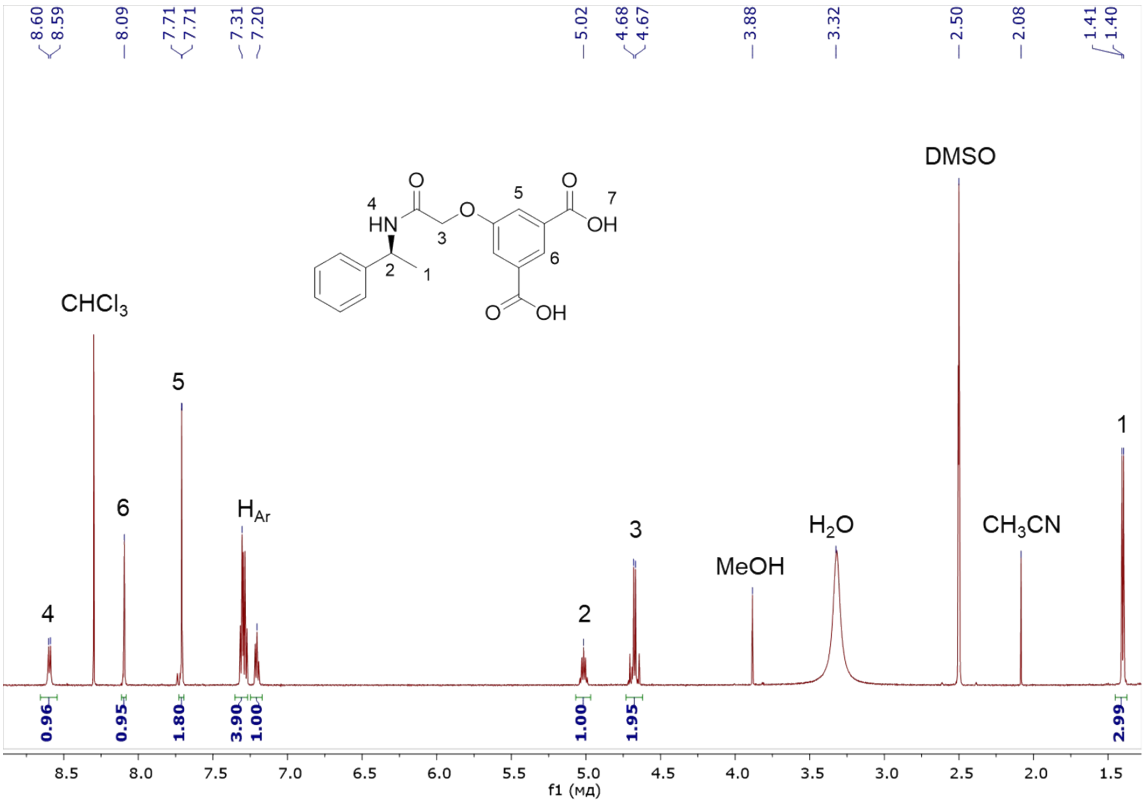

Figure S6. ^{1}H NMR spectrum for **iPHTA-S** (DMSO-d_6, 600 MHz, 25 °C).

2.2 ^{13}C NMR characterization

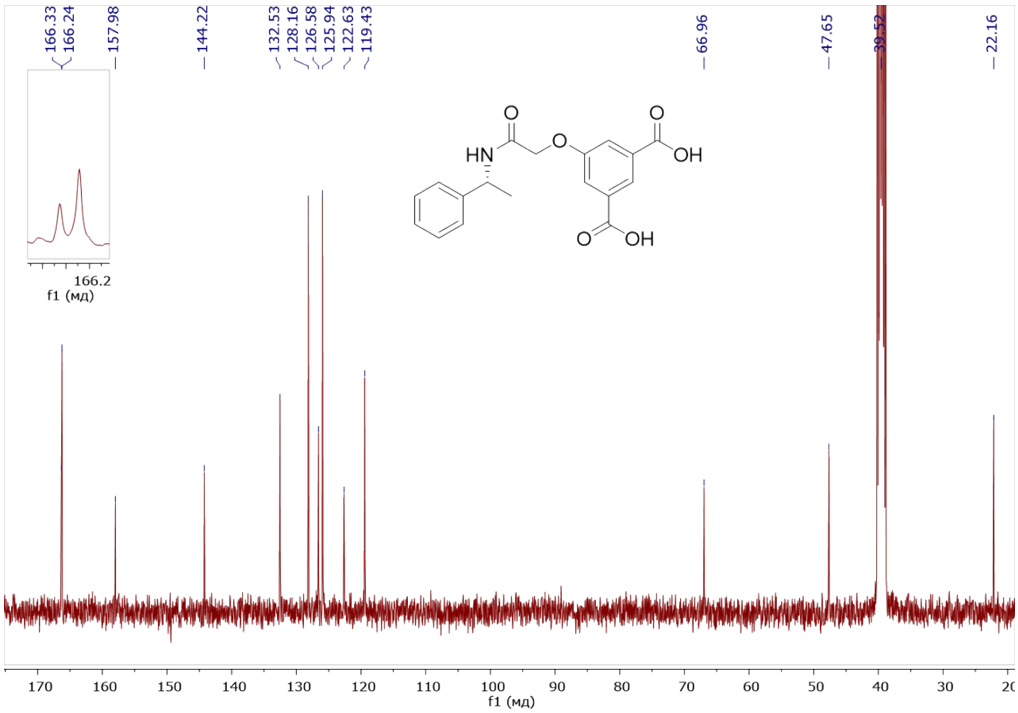

Figure S7. ^{13}C NMR spectrum for **iPHTA-R** (DMSO-d_6, 101 MHz, 25 °C).

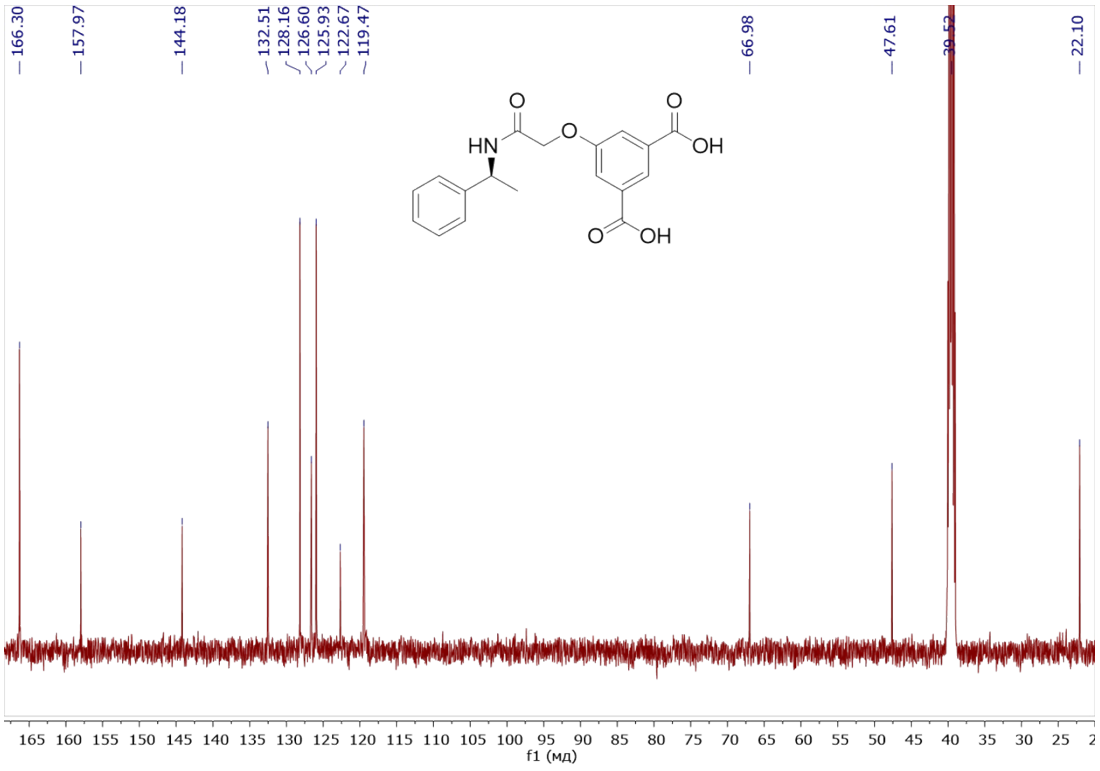

Figure S8. ^{13}C NMR spectrum for **iPHTA-S** (DMSO-d_6, 101 MHz, 25 °C).

2.3 MS characterization

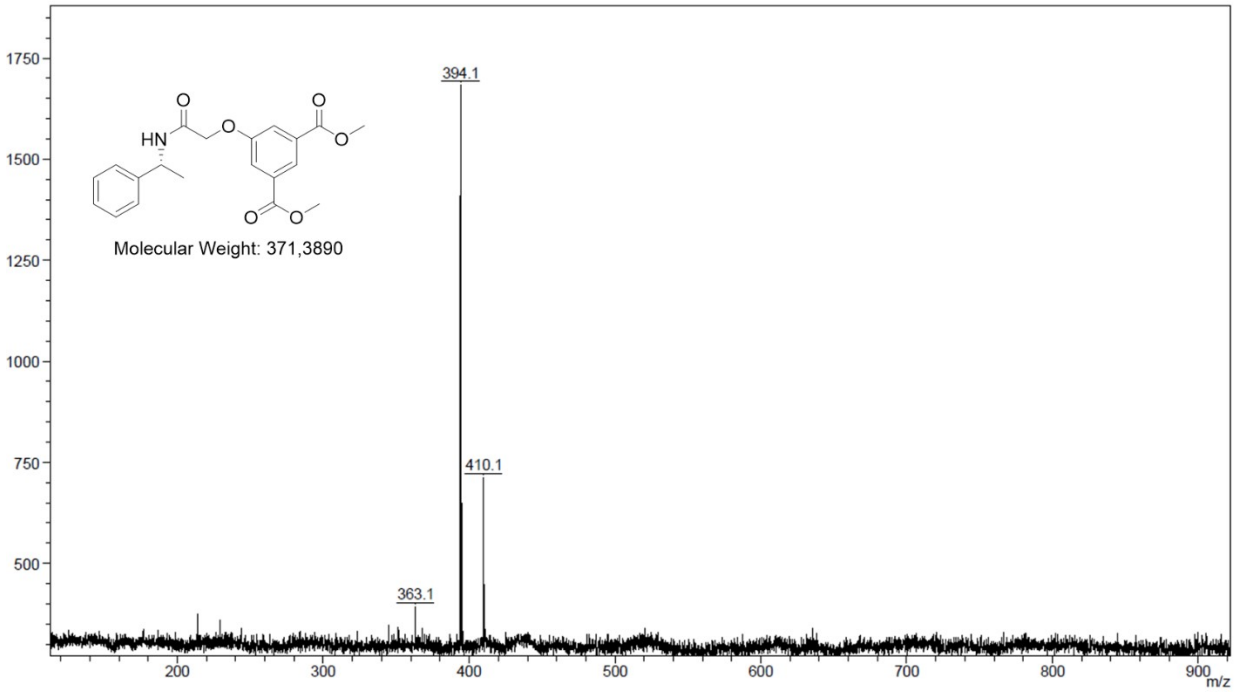

Figure S9. MALDI-MS spectrum for **3-R**.

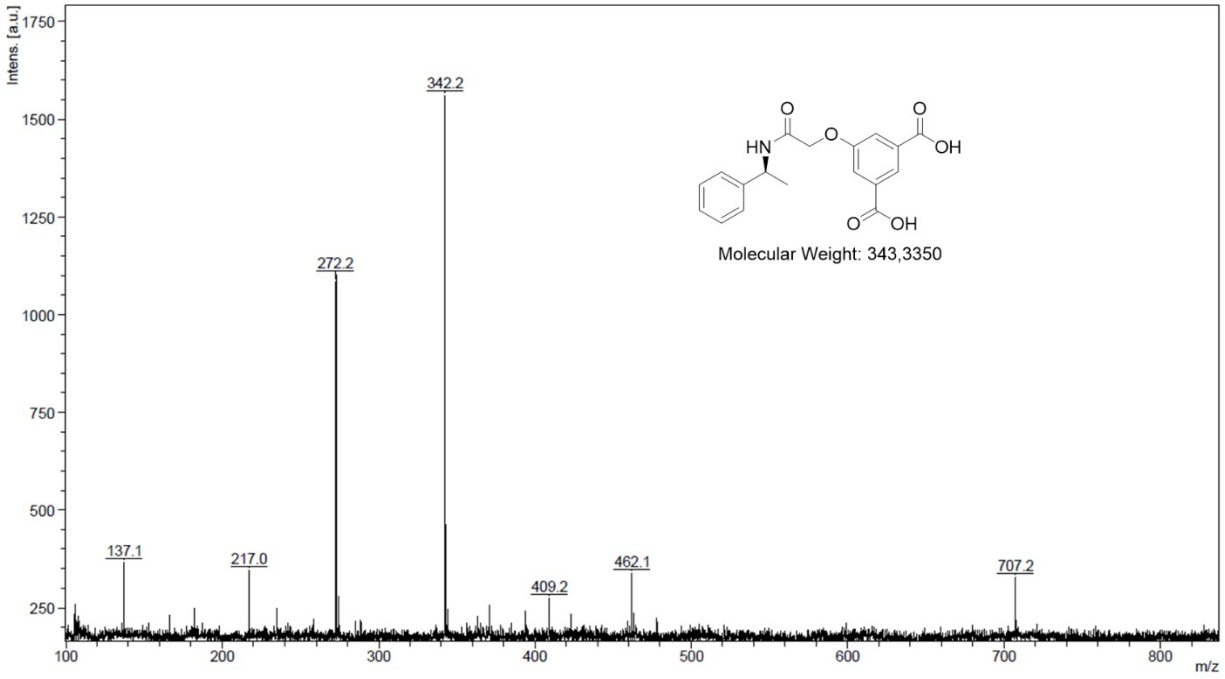

Figure S10. MALDI-MS spectrum for **iPHTA-S**.

2.4 TG/DSC analysis

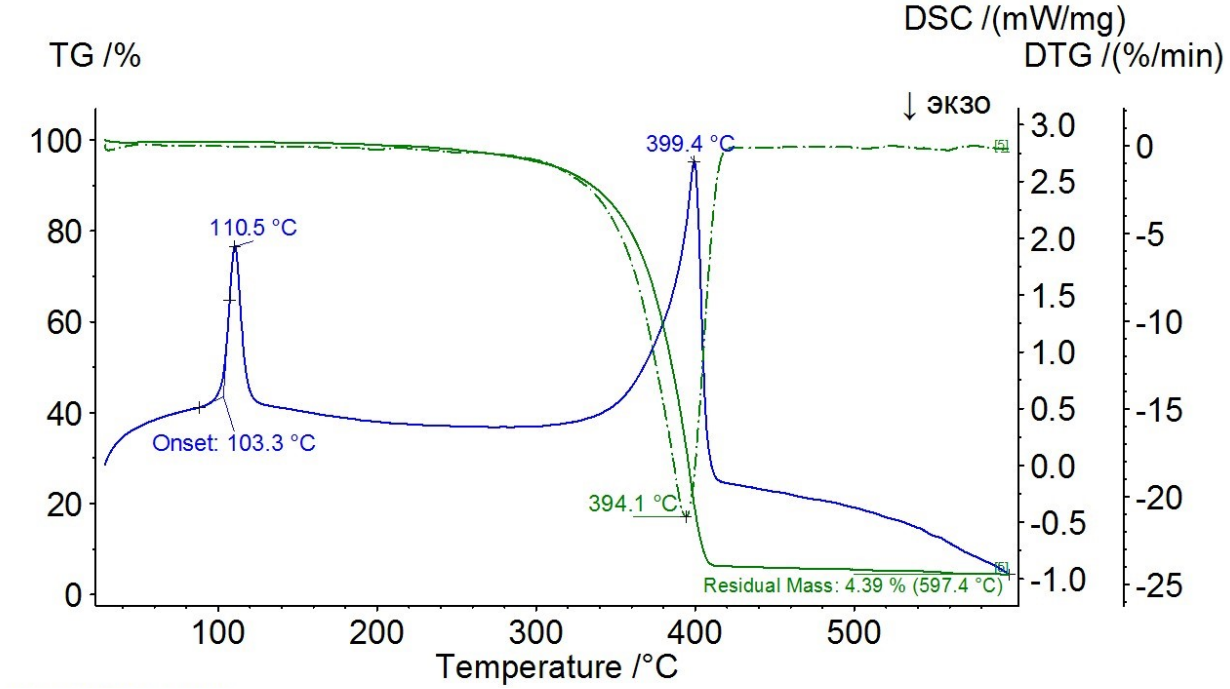

Figure S11. TGA/DSC traces for **3-R**.

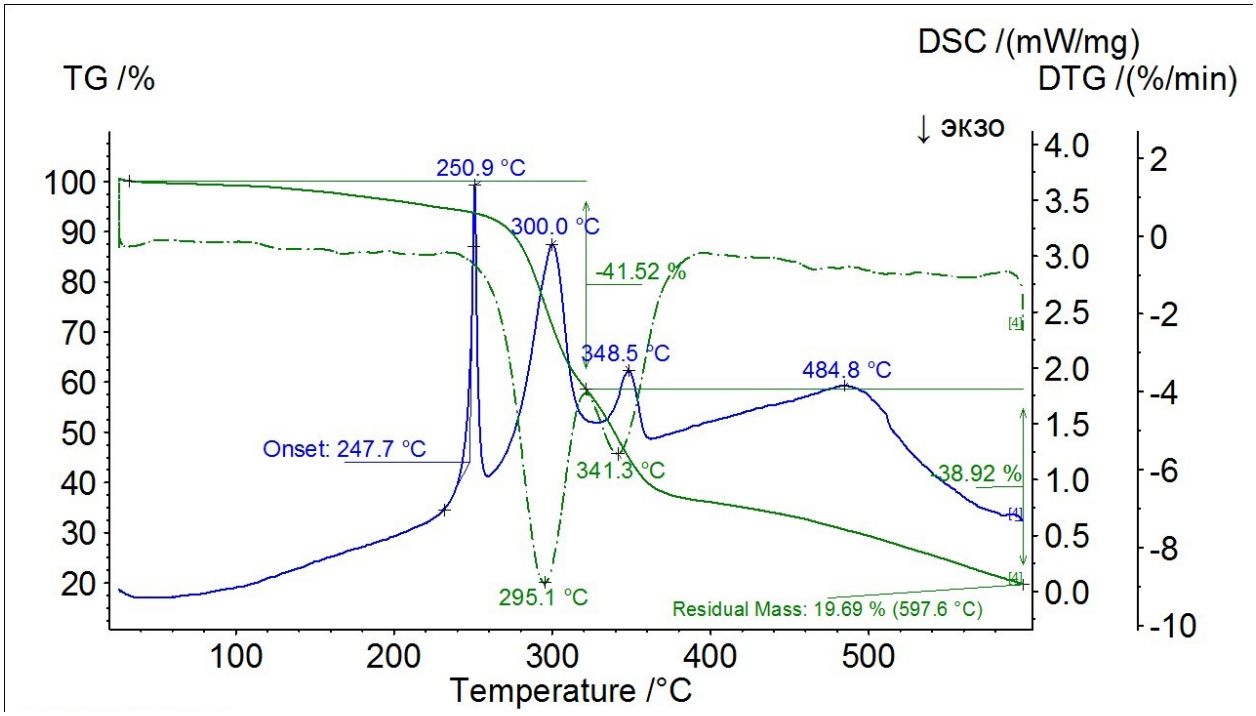

Figure S12. TGA/DSC traces for **iPHTA-R**.

2.5 CD characterization

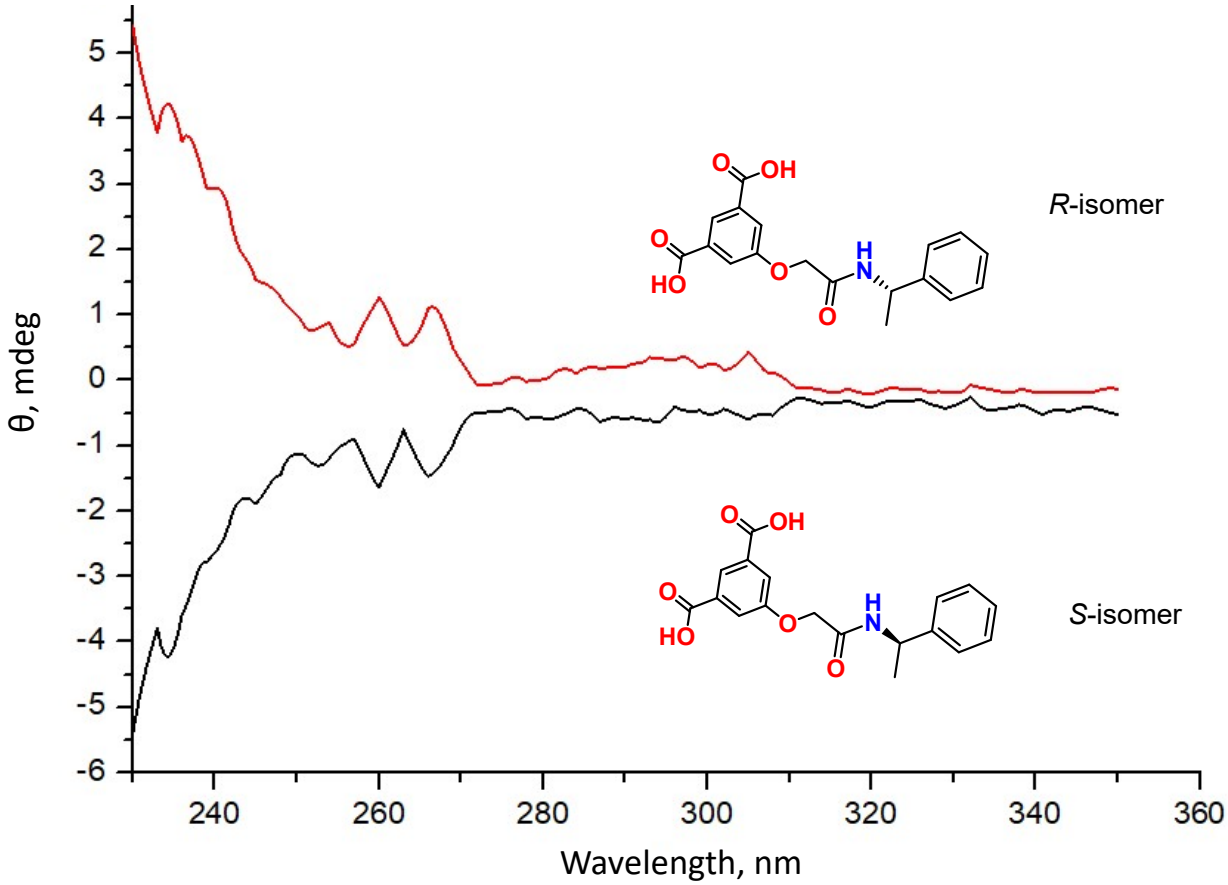

Figure S13. CD spectra for **iPHTA-R** (red line) and **iPHTA-S** (black line) in methanol (C=2.5·10^{-4} M, 25 °C).

3. Synthesis of chiral cages

{[SO_2CA-Co_4(μ_4-H_2O)]$_4$(**iPHTA-R**)$_8$}·solv (**SO_2CA-Co_4-1**): Dicarboxylic acid **iPHTA-R** (20 mg, 0.06 mmol), sulfonylcalix[4]arene **SO_2CA** (25 mg, 0.03 mol), $Co(NO_3)_2 \cdot 6H_2O$ (29 mg, 0.15 mmol) were dissolved in $CHCl_3$ – MeOH mixture (10 ml, V/V=1/1). Triethylamine (41 µl, 0.294 mmol) was added to solution. The resulting mixture was stirred for 1 hour and then filtered off. Dark pink crystals, suitable for X-ray diffraction, were obtained upon slow evaporation after 3 days. Total yield: 37 mg (72%, according to acid **iPHTA-R**). HRESI-MS, m/z: $[M-2H]^{4-}$ calculated for $C_{304}H_{302}Co_{16}N_8O_{100}S_{16}$ 1780.3439, found 1780.3448; deconvoluted mass: [M+2H] calculated for $C_{304}H_{306}Co_{16}N_8O_{100}S_{16}$ 7125.40, found 7125.40; [M+2H+NEt_3] calculated for $C_{304}H_{321}Co_{16}N_9O_{100}S_{16}$ 7226.52, found 7226.52. IR (KBr, cm^{-1}) υ: 3428(m), 2971(s), 2939(s), 2878(w), 2802(w), 2739(m), 2679(s), 2602(w), 2529(w), 2492(m), 1764(w), 1665(m), 1621(m), 1608(s), 1583(m), 1523(m), 1492(s), 1458(s), 1435(s), 1380(s). 1333(m), 1290(m), 1263(m), 1223(w), 1198(w), 1170(w), 1156(w), 1136(m), 1083(m), 1036(m), 967(w), 931(w), 907(w), 838(w), 826(w), 798(m), 779(m), 763(w), 744(w), 726(m), 702(w), 626(m), 590(w), 566(m), 526(w), 494(w), 468(w), 433(w). Elemental Analysis found: C, 51.32 %; H, 4.37 %; N, 1.54 %, calc. for [$C_{304}H_{302}Co_{16}N_8O_{100}S_{16}$]: C, 51.23%; H, 4.33%; N, 1.57%.

SO_2CA-Co_4-2 was synthesized following the same synthetic protocol, described for **SO_2CA-Co_4-1**, excepting **iPHTA-R** was replaced by **iPHTA-S**. Elemental Analysis found: C, 51.30 %; H, 4.34 %; N, 1.59 %, calc. for [$C_{304}H_{302}Co_{16}N_8O_{100}S_{16}$]: C, 51.23%; H, 4.33%; N, 1.57%

3.1 Single crystal X-ray diffraction analysis of chiral cages

The X-ray diffraction data for **SO_2CA-Co_4-1** were obtained on the 'Belok/XSA' beamline (λ = 0.7527 Å, ω-scans) of the Kurchatov Synchrotron Radiation Source (Moscow, Russian Federation). Diffraction patterns were collected using Mardtb goniometer, equipped with Rayonix SX165 2D positional sensitive CCD detector at 100(2) K.[14,15] The frames were recorded with oscillation range of 1°. The data were processed using the XDS program.[16] The multi-scan method was used for absorption correction. The structure was solved with SHELXT[17] and refined by full-matrix least squares on F^2 using the *Olex2* software, [18] which utilises the SHELXL[19] module. Nonhydrogen atoms were refined anisotropically. The hydrogen atoms were placed in calculated positions. The structure was refined using restraints and constraints. The obtained crystallographic data as well as the details of refinement procedure are gathered in Table S1. Unfortunately, a low diffracting ability of many tested crystals precluded the structure refinement using the laboratory X-ray diffractometer. Only synchrotron X-ray radiation source of Kurchatov Institute in Moscow allowed to obtained the reliable solution of obtained crystal structure when only the most ordered molecular fragments, belonging to sulfonylcalix[4]arene-suported {Co_4} clusters as well as the 5-hydroxyisophthalate fragments were identified from the deformation electron density map. Since a high disordering of substituent located at C5 position of benzene ring belonging to isophthalate moieties and solvate molecules was observed in crystal, their positions could not be reliably refined. A Solvent Mask command, generated by the BYPASS module within *Olex2*[18] was used to calculate the residual number of 2048 electrons located within the void of 16008 Å, which can be consistent with the presence of 16 $C_{10}N_1O_1H_{12}$ fragments and 16 $CHCl_3$ solvate molecules, leading to assumed crystal formula $[C_{304}H_{296}Co_{16}O_{100}N_8S_{16}]\cdot 8(CHCl_3)$ of obtained compound. For the exact formula see the TGA data below (Figure S22). The crystallographic data are available for free of charge downloading from the Cambridge Crystallographic Data Centre via www.ccdc.cam.ac.uk/datarequest/cif.

Table S1. Crystallographic data and X-ray structural experiment parameters for **SO_2CA-Co_4-1**.

Compound	**SO_2CA-Co_4-1**
Moiety formula	$C_{224}H_{200}Co_{16}O_{92}S_{16}$, 8[$C_{10}N_1O_1H_{12}$], 8[$CHCl_3$]
Empirical formula	$C_{312}H_{304}Cl_{24}Co_{16}N_8O_{100}S_{16}$
Formula weight	8072.25*
Radiation, wavelength	Synchrotron (λ = 0.7527 Å)
Temperature, K	100(2)
Crystal system	monoclinic
Space group	$P2_1$
a, Å	25.191(5)
b, Å	43.168(9)
c, Å	24.625(5)
β, °	109.29(3)
Volume, Å^3	25274(10)
Z and Z'	2 and 1
Calculated density, g cm^{-3}	1.061 *
Absorption coefficient, mm^{-1}	0.887 *
F(000)	8256.0 *
Crystal size, mm^3	0.3 × 0.2 × 0.2
2θ range for data collection, °	$2.07 \leq 2\theta \leq 40.01$
Index ranges	$-22 \leq h \leq 22$, $-39 \leq k \leq 38$, $-22 \leq l \leq 22$
Reflections collected	90952
Independent reflections	37610
Observed Data [$I > 2\sigma(I)$]	21076
R_{int}	0.0624
R_σ	0.0761
Completeness to θ_{max}, %	94.6

Data / restraints / parameters	37610/6628/2605
Goodness-of-fit on F^2	0.994
Final R indices [$I > 2\sigma(I)$]	R_1 = 0.0861, wR_2 = 0.2252
R indices (all data)	R_1 = 0.1399, wR_2 = 0.2913
Largest diff. peak and hole, e Å^{-3}	1.09 and -0.55
Flack parameter	0.484(9)
CCDC number	2493543

*-assumed values

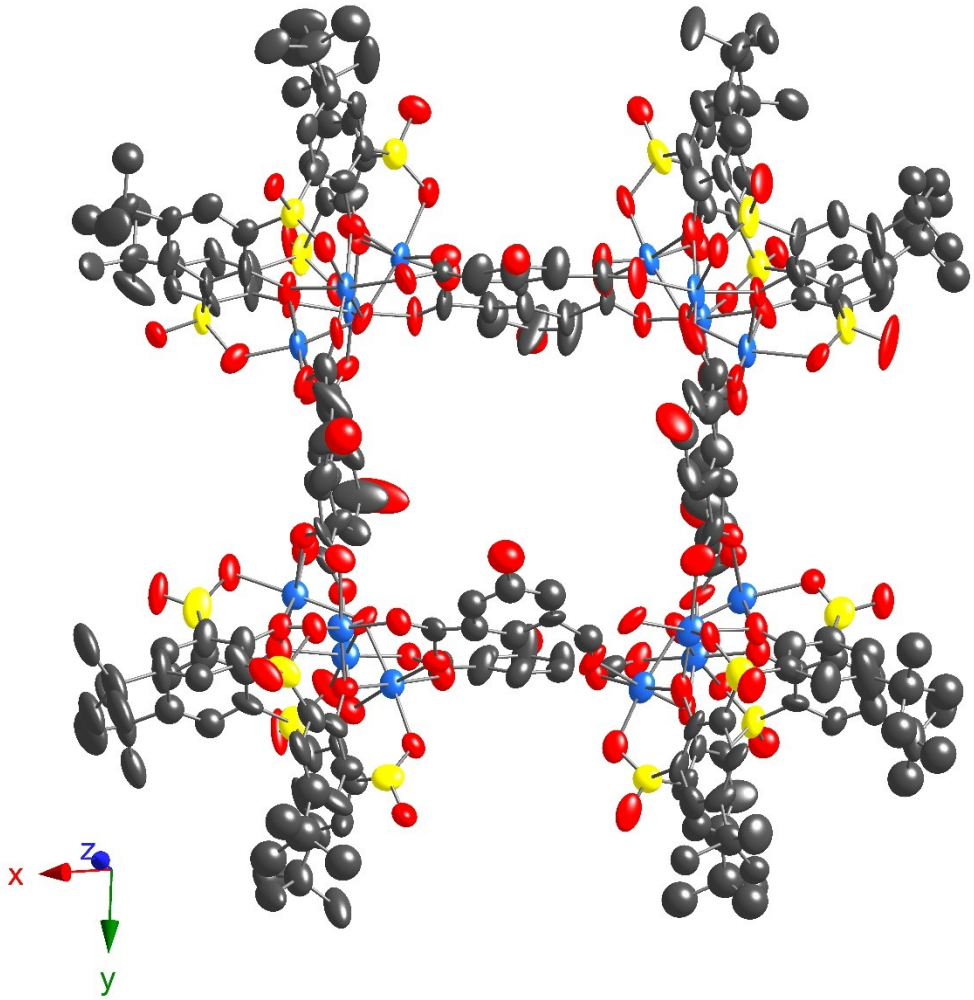

Figure S14. ORTEP view of asymmetric unit for **SO_2CA-Co_4-1**. The C-, O-, S- and Co-atoms are represented by dark grey, red, yellow and light blue thermal ellipsoids (with 30 % probability), respectively. The H-atoms are omitted for clarity.

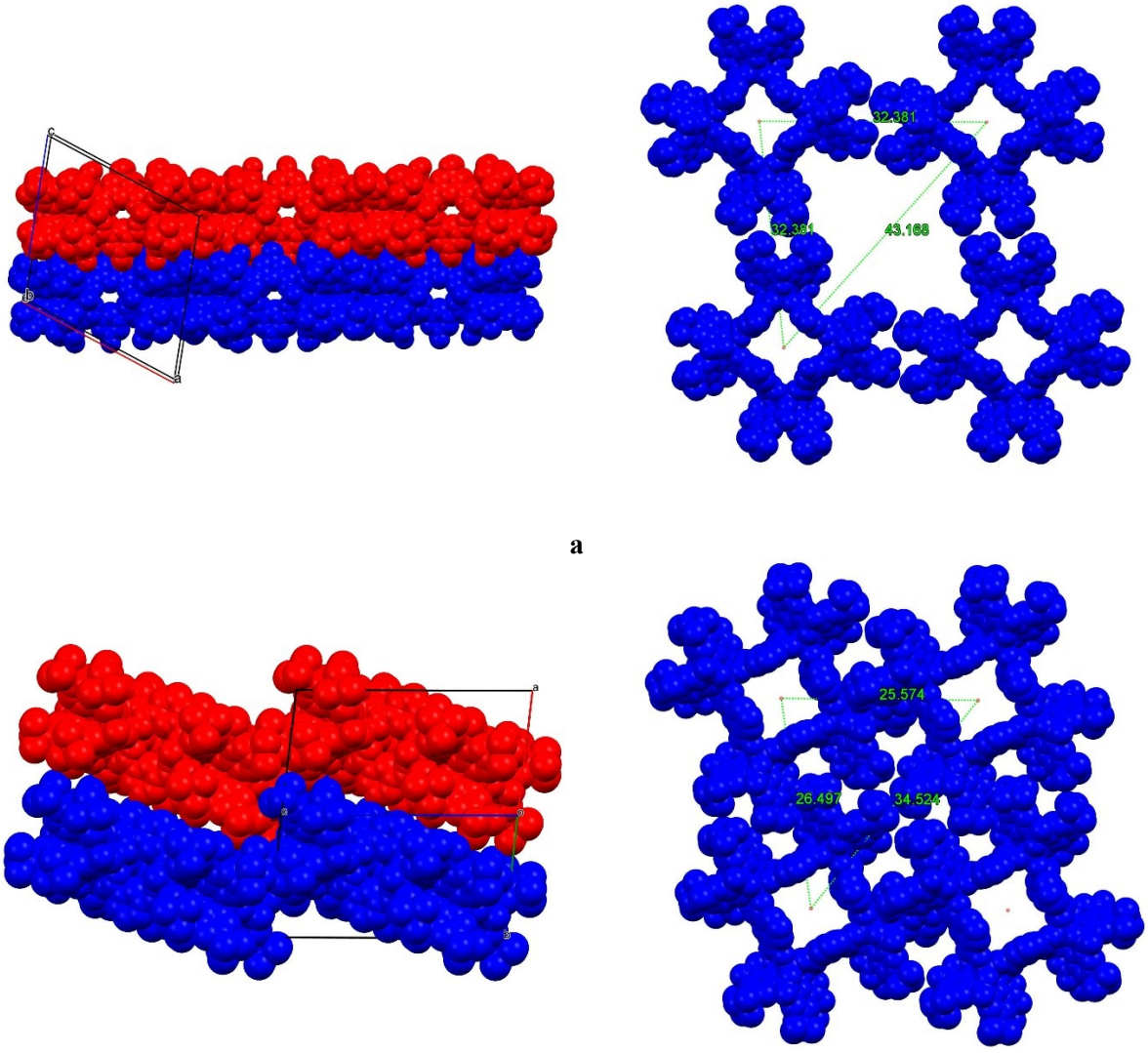

Figure S15. For **SO_2CA-Co_4-1** (a)**,** a fragment of the crystal packing (a), showing the voids formation between within adjacent 2D layers, filled by the highly disordered chiral amide substituents, belonging to isophthalate moieties. The crystal packing for the reported counterpart (b) without any substituents at C5 position of isophtalate moieties.[20]

3.2 Powder X-ray diffraction study of chiral cages

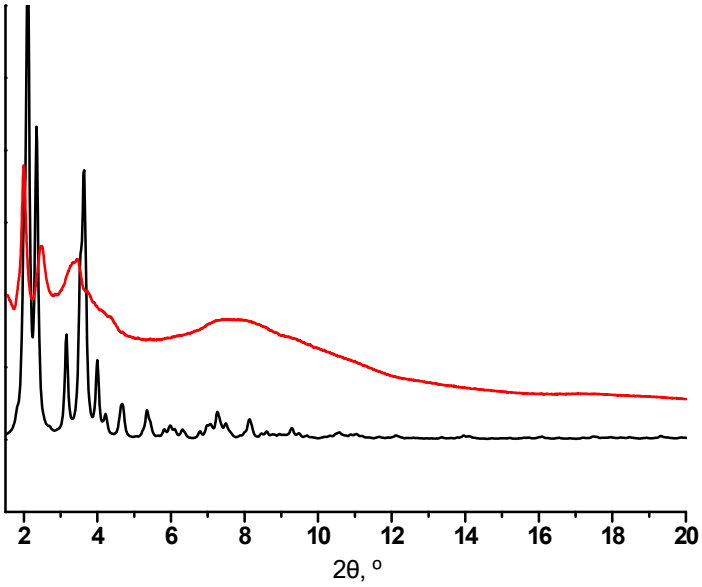

Figure S16. For **SO_2CA-Co_4-1**, a comparison of experimentally obtained (red line) and simulated PXRD patterns (black lines).

3.3 Characterization of chiral cages

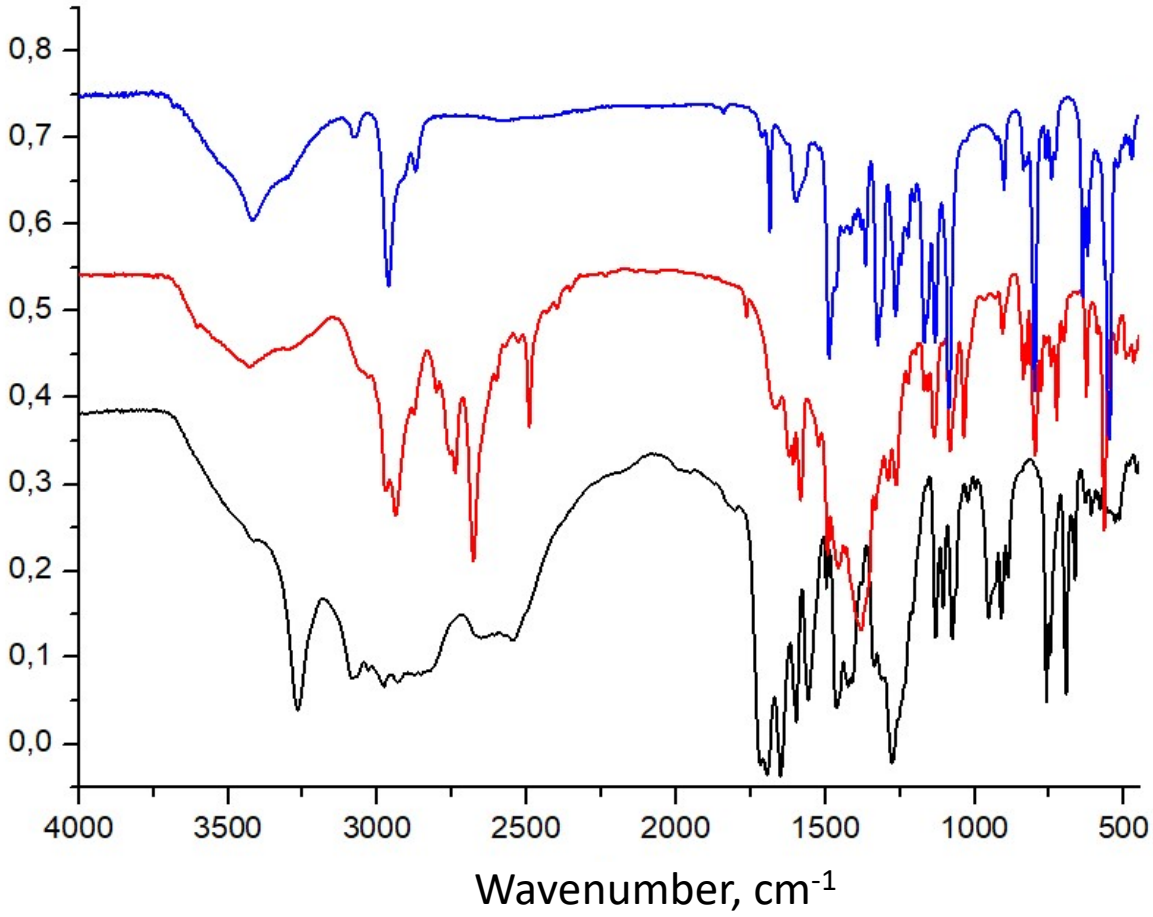

Figure S17. A comparison of IR transmittance spectra of **iPHTA-R** (black line), **SO_2CA-Co_4-1** (red line) and SO_2CA (blue line).

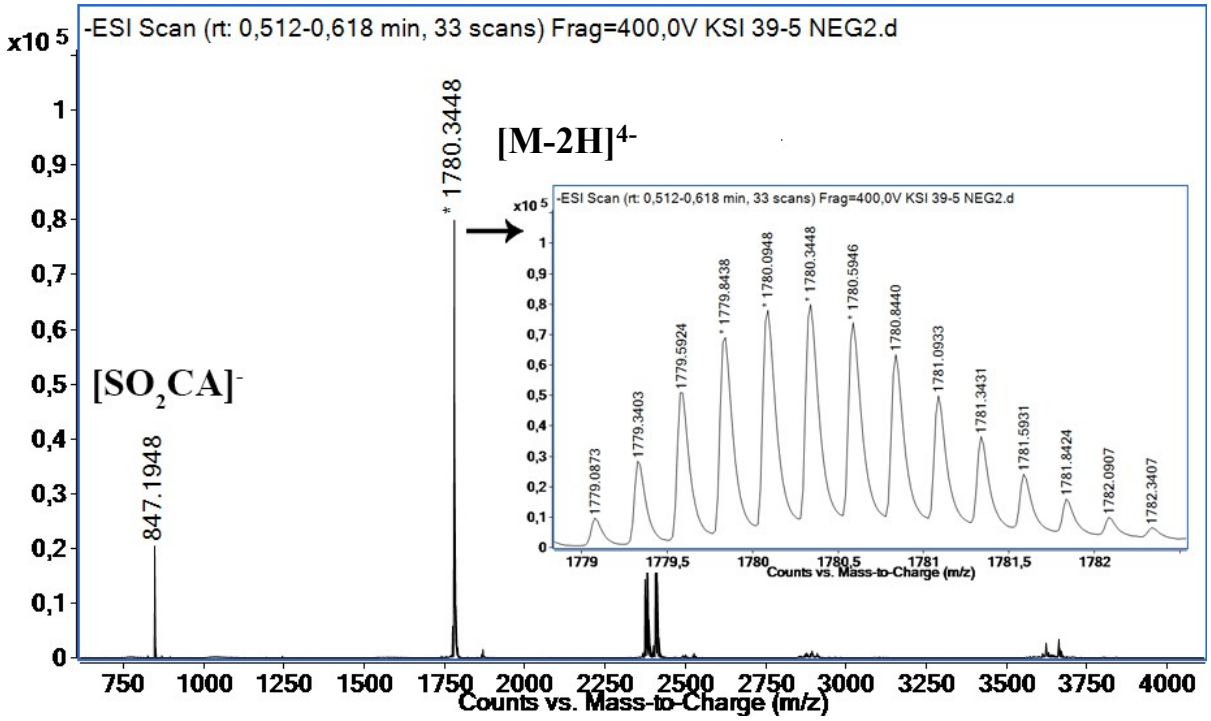

a

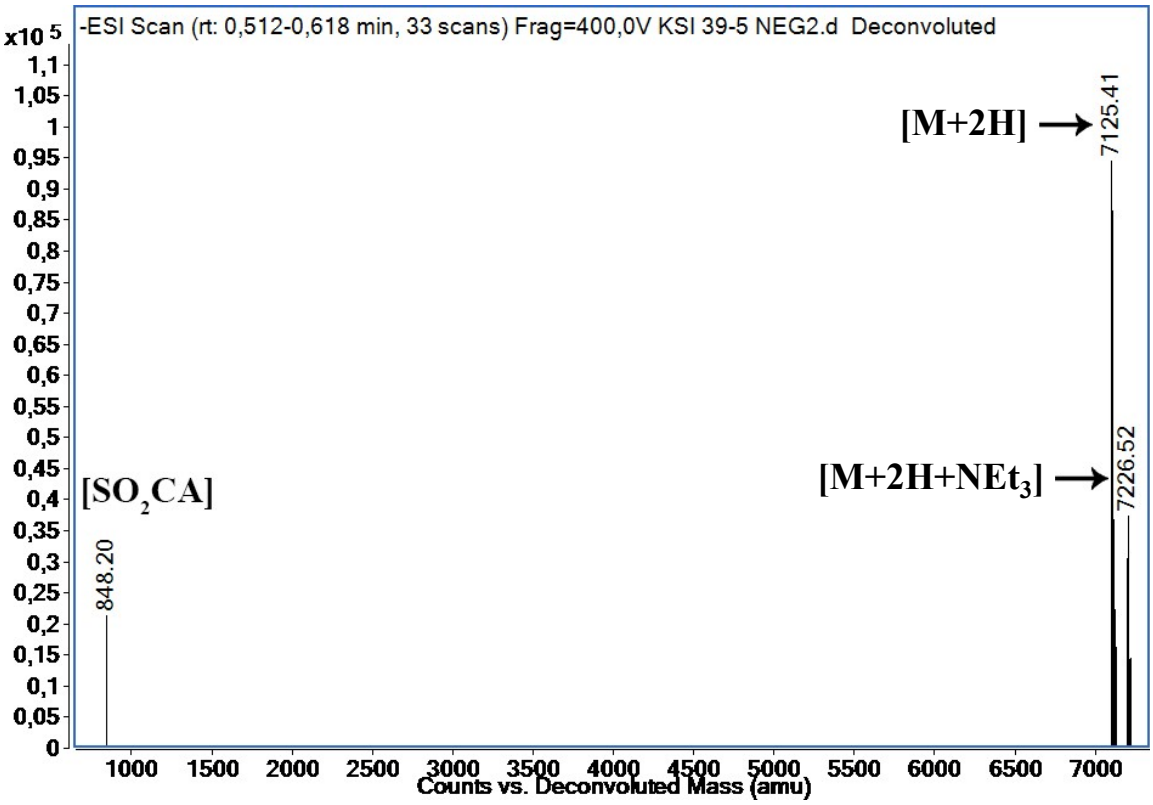

b

Figure S18. HRESI-MS original (A) and deconvoluted spectra of **SO_2CA-Co_4-1.**

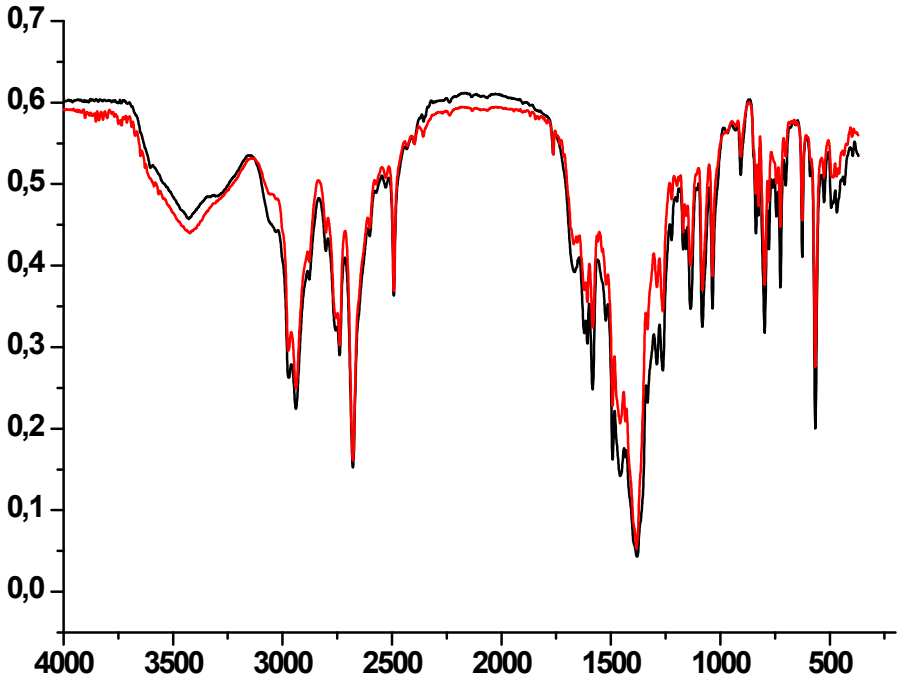

Figure S19. A comparison of IR spectra of **SO_2CA-Co_4-1** (black line) and **SO_2CA-Co_4-2** (red line).

3.4 SAXS study

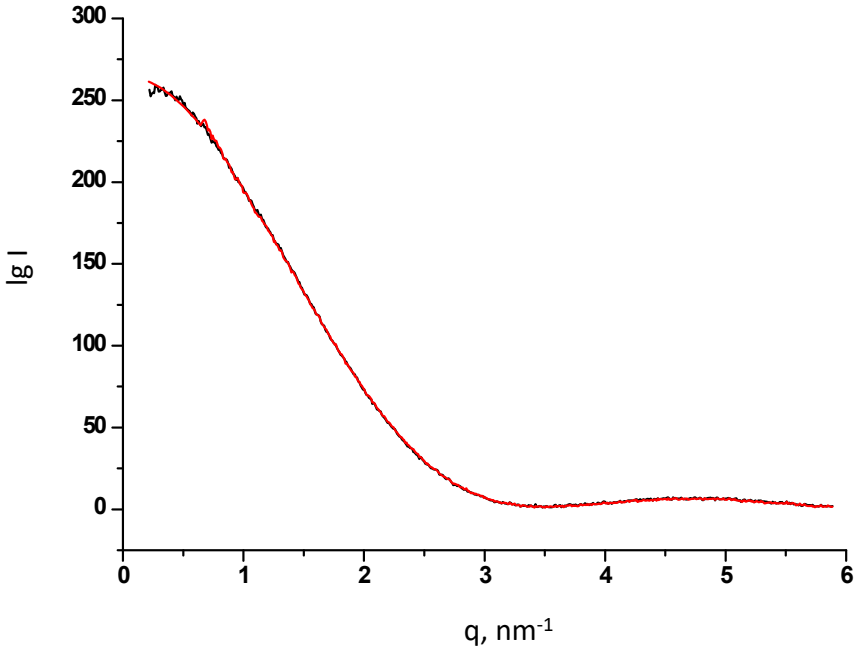

Figure S20. X-ray scattering profile of **SO_2CA-Co_4-1** (black line) and **SO_2CA-Co_4-2** (red line) in THF solution (C = $2.5 \cdot 10^{-4}$ M, 25 °C).

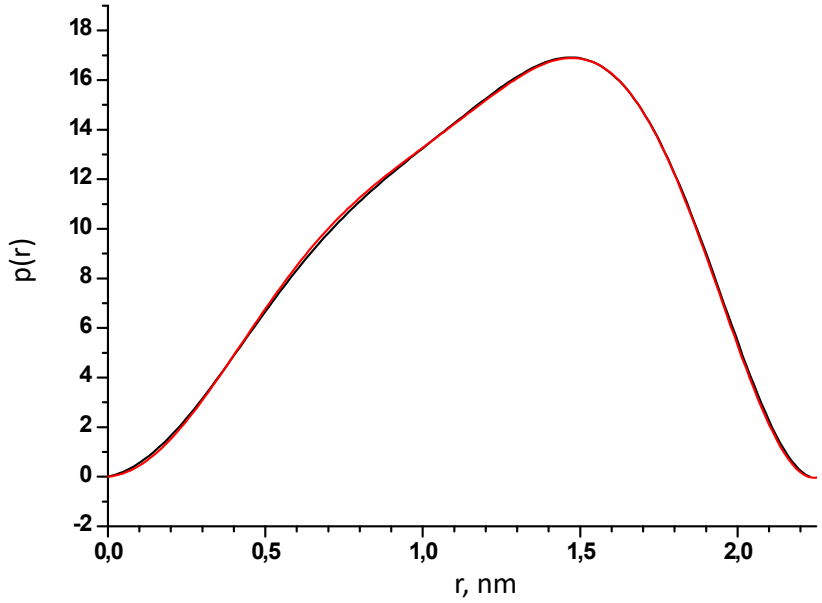

Figure S21. Pair distance distribution function p(r) for **SO_2CA-Co_4-1** (black line) and **SO_2CA-Co_4-2** (red line) in THF solution (C = $2.5 \cdot 10^{-4}$ M, 25 °C).

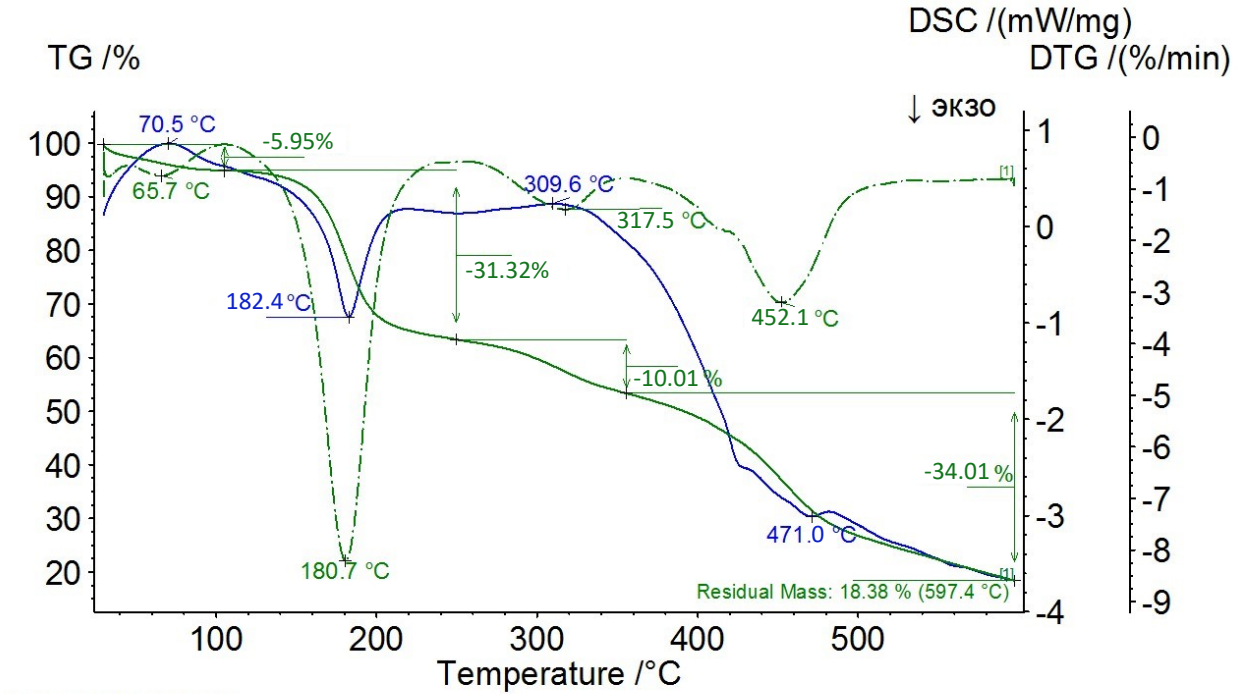

Figure S22. TGA/DSC traces obtained for **SO_2CA-Co_4-1**. The mass-loss of 5.95% was observed in the 25-120 °C temperature range, which is consistent with release of four $CHCl_3$ solvate molecules (calculated mass-loss is equal to 6.28%), affording the correct formula $[C_{304}H_{296}Co_{16}O_{100}N_8S_{16}]\cdot 4(CHCl_3)$ of obtained compound.

4. Guest adsorption study

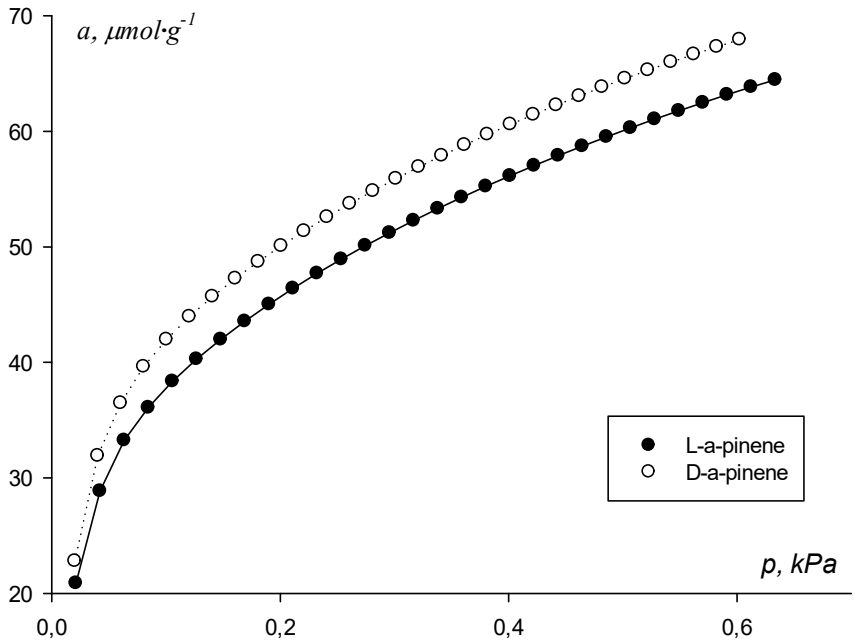

Figure S23. Isotherms of α-pinene adsorption at 90 ˚C on **SO_2CA-Co_4-2**, deposited on the S-DVB polymer matrix.

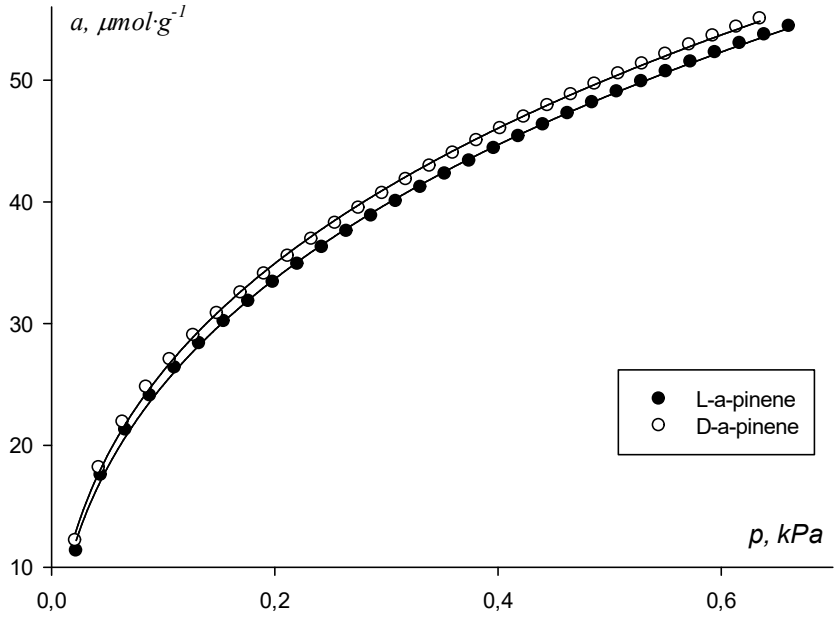

Figure S24. Isotherms of α-pinene adsorption at 85 ˚C on **SO_2CA-Co_4-2**, deposited on the S-DVB polymer matrix.

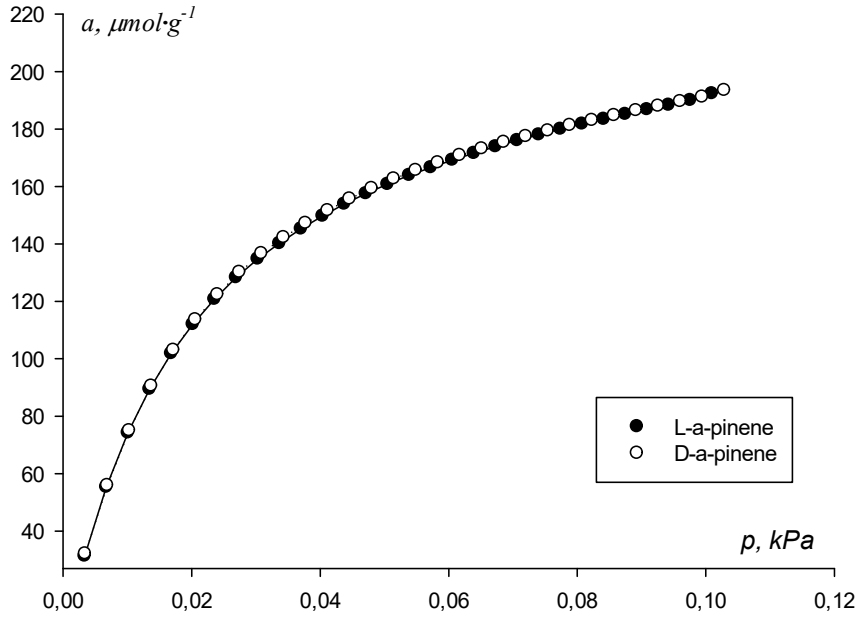

Figure S25. Isotherms of α-pinene adsorption at 90 ˚C on **SO_2CA-Co_4-1**, deposited on the S-DVB polymer matrix.

Table S2. The results of isotherm approximation by Toth equation: a_m – monolayer capacity, μmol·g^{-1}; K_T – Toth constant, Pa^{-1}; t – heterogeneity parameter.

Compound	T, ˚C	L-α-pinene				D-α-pinene			
		a_m	K_T	t	R^2	a_m	K_T	T	R^2
SO_2CA-Co_4-1	85	-	-	-	-	-	-	-	-
SO_2CA-Co_4-2		1352 ± 703	45 ± 15	0.14 ± 0.02	0.9994	1505 ± 766	69 ± 26	0.14 ± 0.02	0.9995
SO_2CA-Co_4-1	90	238 ± 2	48 ± 1	0.93 ± 0.02	0.9998	235 ± 2	48 ± 1	0.96 ± 0.02	0.9998
SO_2CA-Co_4-2		722 ± 450	3604 ± 5403	0.13 ± 0.03	0.9998	-	-	-	-
SO_2CA-Co_4-1	95	182 ± 3	65 ± 2	0.76 ± 0.03	0.9991	176 ± 3	56 ± 2	0.76 ± 0.03	0.9992
SO_2CA-Co_4-2		525 ± 1	0.379 ± 0.005	0.341 ± 0.003	0.9999	593 ± 1	0.348 ± 0.004	0.330 ± 0.002	0.9999

Table S3. The results of isotherm approximation by Dubinin-Radushkevich equation: W_0 – micropore volume, mL·g^{-1}; E – characteristic energy, kJ·mol^{-1}; L_0 – pore diameter, nm; S_m – micropore specific surface area, m^2·g^{-1}.

Compound	T, ˚C	L-α-pinene					D-α-pinene				
		W_0	E	L_0	S_m	R^2	W_0	E	L_0	S_m	R^2
SO_2CA-Co_4-1	85	0.41	21	1	757	0.9807	0.52	20	1	828	0.9809
SO_2CA-Co_4-2		0.13	17	2	121	0.9982	0.12	17	2	124	0.9983
SO_2CA-Co_4-1	90	0.82	18	2	999	0.9700	0.82	18	2	1002	0.9694
SO_2CA-Co_4-2		0.12	20	1	199	0.9956	0.12	20	1	191	0.9964
SO_2CA-Co_4-1	95	0.45	20	1	677	0.9660	0.46	19	1	647	0.9703
SO_2CA-Co_4-2		0.13	13	-	-	0.9990	0.14	13	-	-	0.9988

Table S4. The results of isotherm approximation by Fowler-Guggenheim equation: b – energy of lateral interactions, kJ·mol^{-1}; K_{FG} – Fowler-Guggenheim, Pa^{-1}.

Compound	T, ˚C	L-α-pinene			D-α-pinene		
		b	K_{FG}	R^2	b	K_{FG}	R^2
SO_2CA-Co_4-1	85	0.1	14	0.9611	0.1	14	0.9610
SO_2CA-Co_4-2		2.5	77	0.9864	2.6	66	0.9860
SO_2CA-Co_4-1	90	0.1	21	0.8551	0.1	21	0.8733
SO_2CA-Co_4-2		2.7	26	0.9759	2.5	23	0.9741
SO_2CA-Co_4-1		0.4	17	0.9643	0.3	19	0.9377
SO_2CA-Co_4-2	95	1.5	835	0.9639	1.5	846	0.9605

References

1 *ORGANIKUM. Organisch-chemisches Grundpraktikum*, H. G. Becker, W. Berger, G. Domschke, Deutscher Verlag der Wissenschaften, Berlin, 1965.
2 V. A. Lazarenko, P. V. Dorovatovskii, Y. V. Zubavichus, A. S. Burlov, Y. V. Koshchienko, V. G. Vlasenko, V. N. Khrustalev, *Crystals*, 2017, **7**, 11, 325.
3 R. D. Svetogorov, P. V. Dorovatovskii, V. A. Lazarenko, *Crystal Research and Technology*, 2020, ***55***, 5, 1900184.
4 R. D. Svetogorov, Dionis—Diffraction Open Integration Software, Kurchatov Institute, Moscow, Russia, 2018
5 G. S. Peters, O. A. Zakharchenko, P. V. Konarev, Y. V. Karmazikov, M. A. Smirnov, A. V. Zabelin, E. H. Mukhamedzhanov, A. A. Veligzhanin, A. E. Blagov and M. V. Kovalchuk, *Nucl. Instrum. Methods Phys. Res. A*, 2019, **945**, 162616.
6 G. S. Peters, Y. A. Gaponov, P. V. Konarev, M. A. Marchenkova, K. B. Ilina, V. V. Volkov, Y. V. Pisarevsky and M. V. Kovalchuk, *Nucl. Instrum. Methods Phys. Res. A*, 2022, **1025**, 166170.
7 C. J. Gommes, S. Jaksch and H. Frielinghaus, *J. Appl. Crystallogr.*, 2021, **54**, 1832–1843.
8 A. P. Hammersley, *J. Appl. Crystallogr.*, 2016, **49**, 646–652.
9 K. Manalastas-Cantos, P. V. Konarev, N. R. Hajizadeh, A. G. Kikhney, M. V. Petoukhov, D. S. Molodenskiy, A. Panjkovich, H. D. T. Mertens, A. Gruzinov, C. Borges, C. M. Jeffries, D. I. Svergun and D. Franke, *J. Appl. Crystallogr.*, 2021, **54**, 343–355.
10 A. V. Kiselev and Y. I. Yashin, *Gas adsorption chromatography*, Plenum Press, New York, 1969.
11 C. Nguyen and D. D. Do, *Carbon*, 2001, **39**, 1327 –1336.
12 D. Dollimore and G. R. Heal, *Surf. Technol.*, 1978, **6**, 231-258.
13 A. Mondal, G. K. Barik, S. Sarkar, D. Mondal, M. Ahmad, T. Vijayakanth, J. Mondal, M. K. Santra, P. Talukdar, *Chem. Eur. J.* 2023, 29, e202202887.
14 V. A. Lazarenko, P. V. Dorovatovskii, Y. V. Zubavichus, A. S. Burlov, Y. V. Koshchienko, V. G. Vlasenko, V. N. Khrustalev, *Crystals*, 2017, *7*, 11, 325.
15 R. D. Svetogorov, P. V. Dorovatovskii, V. A. Lazarenko, *Crystal Research and Technology*, 2020, ***55***, 5, 1900184.
16 W. Kabsch, *Acta Crystallogr*., 2010, **D66**, 125.
17 G. M. Sheldrick, *SHELXT* – Integrated space-group and crystal-structure determination, *Acta Crystallogr. Sect. A*, 2015, **71**, 3–8.
18 O. V. Dolomanov, L. J. Bourhis, R. J . Gildea, J. A. K. Howard, H. J. Puschmann, *Appl. Cryst.,* 2009, **42**, 339.
19 G. M. Sheldrick, Crystal Structure Refinement with SHELXL, *Acta Cryst. Sect. C*, 2015, **71**, 3–8.
20 F.-R. Dai, D. C. Becht and Z. Wang, *Chem. Commun.*, 2014, **50**, 5385–5387.